

---

## Time-Resolved Crystallography: Principles, Problems and Practice [and Discussion]

Keith Moffat, Ying Chen, Kingman Ng, Duncan McRee, Elizabeth D. Getzoff, M. Rossmann, J. Hajdu and G. A. Petsko

*Phil. Trans. R. Soc. Lond. A* 1992 **340**, 175-190  
doi: 10.1098/rsta.1992.0059

---

### Email alerting service

Receive free email alerts when new articles cite this article - sign up in the box at the top right-hand corner of the article or click [here](#)

---

To subscribe to *Phil. Trans. R. Soc. Lond. A* go to:  
<http://rsta.royalsocietypublishing.org/subscriptions>

---

# Time-resolved crystallography: principles, problems and practice

BY KEITH MOFFAT<sup>1</sup>, YING CHEN<sup>1</sup>, KINGMAN NG<sup>1</sup>, DUNCAN MCREE<sup>2</sup>  
AND ELIZABETH D. GETZOFF<sup>2</sup>

<sup>1</sup>*Department of Biochemistry and Molecular Biology, The University of Chicago, 920 E. 58th Street, Chicago, Illinois 60637, U.S.A.*

<sup>2</sup>*The Scripps Research Institute, Department of Molecular Biology MB4, 10666 N. Torrey Pines Road, La Jolla, California 92037, U.S.A.*

Time-resolved crystallography is founded on the belief that a complete understanding of mechanism at the molecular level demands knowledge, not just of long-lived, readily observable structures, but also of short-lived intermediates in processes such as catalysis, ligand binding and release, and protein unfolding. Synchrotron X-ray sources enable X-ray diffraction patterns of high quality to be obtained from single crystals with exposure times that are often commensurate with the lifetime of the desired intermediates. The basic tools are therefore in place. How shall they be applied effectively? Can crystallography, long regarded as a static technique, in fact encompass dynamic processes? What pitfalls remain to be overcome?

A time-resolved crystallographic experiment has five main components: the X-ray source; reaction initiation; reaction monitoring by optical or other techniques; X-ray data acquisition in real time; and data reduction and analysis. These are illustrated by our recent work on photoactive yellow protein, and on the acquisition and analysis of crystallographic data using 120 ps exposures.

## 1. Introduction

Modern structural biology at the molecular level has two main thrusts: the study of structure for its own sake, as in protein folding; and the study of structure as a foundation for an understanding of mechanism, as in enzymology. Despite the enormous successes of three decades of X-ray crystallography in determination of macromolecular structure, determination of mechanism has proved more challenging by far. Why is the link between structure and mechanism, which we firmly believe exists, so hard to elucidate? We believe it is in part because structure determination has been exclusively static, based on a time average over the lengthy duration of a conventional X-ray experiment and a space average over all the molecules in a crystal, some  $10^{12}$ – $10^{14}$ . But mechanism involves inherently dynamic events: the interconversion of chemical species in catalysis, the binding and release of oxygen from haemoglobin, or calcium from calmodulin, or antigen from antibody, or virus from cell surface receptor. Thus we as crystallographers have been forced to extrapolate from our static images to the dynamic but hitherto invisible images of transient species which are crucial to mechanism. This limitation was foreseen just after the first structure determination of an enzyme, lysozyme, when Gutfreund &

*Phil. Trans. R. Soc. Lond. A* (1992) **340**, 175–190

Printed in Great Britain

© 1992 The Royal Society

[ 7 ]

175

Knowles (1967) wrote: ‘... the mechanism of enzyme catalysis will [not] be completely solved by X-ray analysis of the crystal structure of the proteins and their compounds (making a model of a horse from photographs does not necessarily tell us how fast it can run)...’. Their reference to photography of horses harks back to the nineteenth century photographer Eadweard Muybridge who attacked a long-standing problem in animal locomotion: how does a horse gallop? He did so by devising an early form of movie camera and with it took a series of images closely spaced in time as a horse galloped past trip wires set to trigger the camera shutters. Thus he adapted still photography to reveal motion and applied it to a physiological problem. We continue to face the Gutfreund & Knowles problem today: how do our molecular horses run, and why do they run so fast? Like Muybridge, our answer depends on new apparatus and techniques; and again like Muybridge, the response is easier if the processes are slower. Trotting is easier to understand than galloping.

It is worth re-emphasizing the assumptions on which the proposals for time-resolved crystallography are based. First, the X-ray diffraction pattern obviously must be retained throughout the structural process, so that quantitative measurements of the time-dependent X-ray intensities can be made. This demands isomorphism but, as Schulz (1991) has re-emphasized, many processes involve substantial domain motion or other large-scale tertiary and quaternary structural changes. Time-resolved crystallography is therefore likely to be confined to those systems where the tertiary structural changes are sufficiently large to be detectable, yet not so large as to disrupt the crystal lattice. As a rule of thumb, the faster a process, the smaller the underlying structural change; local tertiary structural changes such as aromatic side chain rotation are typically faster than large-scale tertiary changes, which in turn are faster than quaternary changes. Fast time-resolved crystallography may in some respects be more widely applicable than slow.

Secondly, structural intermediates can only be detected if they accumulate appreciably, and if their lifetime is longer than the minimum X-ray exposure time. The lifetime and population of intermediates can be manipulated by experimental conditions such as temperature, pH, the presence or absence of effectors and inhibitors, and by site-specific mutagenesis of the native protein in a manner designed to alter substantially its kinetic parameters. A further problem arises if there is a multiplicity of parallel pathways, no one of which is ever well-populated, rather than the structurally unique pathway generally assumed.

Thirdly, the time-dependent changes in X-ray intensities must be reducible to structure amplitudes and thence to electron density and atomic structures. This seems obvious, but at its heart lies the nature of the X-ray diffraction process from a heterogeneous crystal which at a minimum exhibits time-dependent substitutional disorder. The nature of this disorder, and in particular whether it is spatially random in the crystal (no correlation of conformation between adjacent molecules), and whether it is accompanied by other forms of lattice disorder (such as gradients in cell dimensions) is critical, but poorly understood.

We now consider the five main components of a time-resolved experiment: the X-ray source, reaction initiation, optical or other monitoring of the crystal, X-ray monitoring, and data analysis. Since time-resolved crystallography has been reviewed in some detail (Moffat 1989; Hajdu & Johnson 1990) we will emphasize more recent developments and in particular, those challenges that arise when considering intermediates with lifetimes well under one second. The timescales and structural processes with which we shall be concerned are displayed in figure 1.

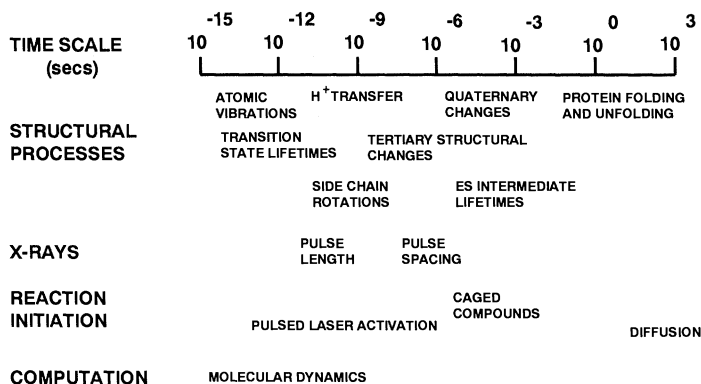


Figure 1. Timescales and processes in time-resolved crystallography. Adapted from figure 1 of Moffat (1989).

## 2. The time-resolved experiment

### (a) X-ray source and optics

With the exception of a few very slow reactions spanning one or more hours which can be probed with laboratory sources (Wyckoff *et al.* 1967), time-resolved experiments use intense synchrotron sources, either bending magnets, wigglers or undulators (Margaritondo 1988; Helliwell 1992). The first two emit relatively smooth spectra but the third emits a strongly featured spectrum in which much of the X-ray power is concentrated near a few energies, the harmonics of a fundamental energy. Further, both the intensity and the shape of an undulator spectrum vary substantially with position relative to the axis of the undulator. An undulator X-ray beam is extremely highly collimated and well-matched to the small size of macromolecular crystals and their requirement for high angular collimation. All synchrotron sources are naturally polychromatic and therefore appropriate to the Laue technique (Amorós *et al.* 1975; Wood *et al.* 1983; Moffat *et al.* 1984; Helliwell 1985; Hajdu *et al.* 1987). The exposure time in a Laue experiment is inversely proportional to the spectral intensity falling on the crystal, in units such as photons  $(\text{s mm}^2 0.1\% \text{ bandpass})^{-1}$ . This quantity is higher for undulator sources at the peaks of the harmonics than for wigglers, and further enhanced for both types of source by focusing. A broad incident wavelength spectrum stimulates a larger volume of reciprocal space in one image, proportional to  $\lambda_{\text{max}} - \lambda_{\text{min}}$ , and hence reduces the total number of images required in a data-set. It does not affect the Laue exposure time which depends solely on the spectral intensity. A broad spectrum, however, enhances radiation damage and thermal artifacts (see §2*d*) and increases the background around each Laue reflection (Moffat *et al.* 1989). These may prove to be serious limitations.

The X-ray power delivered by wigglers and undulators on the third generation hard X-ray sources under construction, the APS and the ESRF, is so high that it is a major challenge to design monochromators and focusing elements which will not merely withstand the heat load imposed by the X-ray beam, but retain their optical properties (see for example Smither & Freund 1990). Further, time-resolved experiments demand stability since they depend on the measurement of small differences in scattered intensities as a function of time. If the incident intensity fluctuates due to source motion, thermal degradation of the optics or mechanical

Table 1. Observed and projected spectral intensities for Laue beam lines, near 1 Å

beam line	source	spectral intensity photons/(s mm <sup>2</sup> 0.1 %)	spectral intensity per bunch photons/(mm <sup>2</sup> 0.1 %)
Daresbury SRS 9.5	wiggler	$2 \times 10^{12}$ (a)	$2 \times 10^4$ (b)
NLSL X26C	dipole	$3 \times 10^{12}$ (c)	$5 \times 10^4$ (d)
CHESS C2	dipole	$1 \times 10^{11}$ (e)	$2 \times 10^5$ (f)
CHESS A3	undulator	$1 \times 10^{13}$ (g)	$1 \times 10^7$ (h)
APS	undulator A	$7 \times 10^{14}$ (i)	$1 \times 10^8$ (j)
ESRF	wiggler	$2 \times 10^{15}$ (k)	$4 \times 10^8$ (l)

(a) 5T, 3 pole wiggler with Pt coated, focusing toroid. Assumes SRS operation at 200 mA. Adapted from table 5.5 of Helliwell (1992). (b) As in (a); assumes 5 mA operation. (c) Dipole with Pt coated, focusing cylinder. Assumes NLSL operation at 200 mA. (d) As in (c); assumes 5 mA operation. (e) Dipole, unfocused. Assumes CESR operation at 80 mA. See fig. 5.2 of Shenoy *et al.* (1988). (f) As in (e); assumes 32.5 mA operation. (g) APS prototype for undulator A. CESR operated in dedicated, low emittance mode. Value is for the peak of the third harmonic at 0.97 Å. Assumes operation at 80 mA. See Bilderback *et al.* (1989) and Szebenyi *et al.* (1992). (h) As in (g); assumes 32.5 mA operation. (i) Projected value; on axis at 50 m with no focusing. Assumes APS operation at 100 mA. See fig. 6.7 of Shenoy *et al.* (1988). (j) As in (i); assumes 5 mA operation. (k) Projected value; 44 pole wiggler source with 1.3 m toroidal focusing mirror, at 20 keV. Assumes ESRF operation at 100 mA. The focal spot size is 0.033 mm<sup>2</sup>. Adapted from Wulff (1991). (l) As in (k); assumes 7.5 mA operation.

jitter in the beam line components, the experiment is seriously compromised. The optimum source and beam line configuration for fast time-resolved experiments is therefore not yet established. We show below (Szebenyi *et al.* 1992, and §3b) that quite accurate structure amplitudes can be extracted, even from the sharply featured spectrum emitted by undulator sources.

All synchrotron X-ray sources are pulsed. The duration of an individual X-ray pulse derived from a single bunch of electrons or positrons is around 100 ps. The inter-pulse spacing may be as long as the circulation time of a single bunch, typically 1–3 μs (or a sub-multiple thereof if multiple bunches are employed). An X-ray experiment may be classed according to the number of pulses needed. A single-pulse experiment and a multi-pulse stroboscopic experiment have an X-ray time resolution given by the pulse length; a multi-pulse conventional experiment has a time resolution given by the number of pulses multiplied by the inter-pulse spacing. The first two classes of experiment therefore offer a time resolution several orders of magnitude better than the third. However, stroboscopic experiments require a fully reversible system, which can only be achieved if crystal damage due to both X-ray absorption and reaction initiation is minimal and if the chemistry of the system is suitable; and single-pulse experiments require an extremely intense source, efficient optics, and a strongly scattering crystal (see §3b below).

Table 1 presents spectral intensities observed and projected for various synchrotron beam lines.

#### (b) Reaction Initiation

Successful reaction initiation is arguably one of the largest challenges in a time-resolved experiment. Initiation must be rapid with respect to the reactions under study; synchronizable with X-ray data collection; benign to the crystals; reproducible; and uniform throughout the crystal. Initiation can be achieved by either chemical means such as a diffusion- or light-induced change in concentration of a

reactant or essential cofactor, or by physical means such as a temperature or pressure jump. For rapid reactions, initiation by light using well-developed pulsed or CW laser technologies is likely to be the method of choice. However, the more rapid the reaction, the higher the peak laser power that must be applied to the crystal and the greater the likelihood of damage. Classic examples of a naturally photosensitive system are CO complexes of haemoglobin and myoglobin (Parkhurst & Gibson 1967), and of a system on which photosensitivity can be conferred by ingenious chemistry, caged ATP (Kaplan *et al.* 1978; McCray & Trentham 1989). These and other examples appear elsewhere in this volume.

Reaction initiation is often observed to be accompanied by a transient increase in apparent crystal mosaicity, or even complete loss of the diffraction pattern. The surprise is perhaps that crystalline order returns, rather than its initial disappearance; and this suggests that the origin of the loss of order may be in part due to physical effects rather than chemical. The time course of the alteration in apparent mosaicity is important: does it coincide with the build up and decay of a particular species? If so, then it may be intrinsic to the experiment: the structure of that species is incompatible with the initial (and final) crystal lattice. Alternatively, does it coincide with a candidate physical process, such as equilibration of a thermal or concentration gradient? If so, it is artefactual and may be minimized by careful experimental design.

Reaction initiation by a laser invariably leads to crystal heating. We discuss in §3*a* below an explicit model for the generation of thermal gradients in crystals of photoactive yellow protein (PYP). For a typical  $(200\ \mu\text{m})^3$  protein crystal,  $350\ \mu\text{J}$  uniformly absorbed and converted to heat will raise its temperature by  $10\ ^\circ\text{C}$ . Suppose instead that this heating is very non-uniform and is concentrated at the front face of the crystal struck by the laser, due to an extremely high optical density of the crystal. How long will it take for thermal equilibration and dissipation of this thermal gradient to occur? The thermal diffusion time  $t$  in which the temperature at the back of the crystal changes by a fraction, approximately  $1/e$ , of the (assumed fixed) temperature difference, is given by

$$t \approx L^2 \rho C_p / 4k_T,$$

where  $L$  is the crystal thickness,  $\rho$  the density,  $C_p$  the heat capacity per unit mass at constant pressure, and  $k_T$  the thermal conductivity. Inserting values for water and as a guide taking  $L = 200\ \mu\text{m}$ , then  $t = 67\ \text{ms}$ , which suggests that complete equilibration spanning several thermal diffusion times will take a few hundred milliseconds. Of equal importance, for times less than about  $25\ \text{ms}$ , essentially no thermal equilibration can take place. The real situation is considerably more complicated: the crystal is in thermal contact with a capillary wall and mother liquor, bathed in a gas stream, and heated non-uniformly but throughout its thickness. Also, thermal gradients may give rise to structural gradients and changes in cell dimensions; their dissipation may occur on a different timescale. However, the calculation serves as a rough guide. For PYP, preliminary studies suggest that changes in apparent mosaicity do occur on this timescale, after turning off a CW laser (see §3*a*).

### (c) *Optical monitoring*

Before doing a time-resolved experiment, it is essential that the nature of the biological activity in the crystal – and even its existence – be established by optical or other means. At a minimum, the rate constants for interconversion of optically

detectable intermediates in the crystal must be determined, together with their dependence on other factors which may be manipulated such as temperature, nature of the solvent, and the concentration of inhibitors and effectors. It is of concern that few crystals have had their activity characterized in this way (Makinen & Fink 1977). A structural interpretation of activity may be advanced on the basis of crystal structures whose activity is qualitatively different from that in free solution, or at worst completely absent.

Most kinetic studies are carried out in solvents which are distinctly different from those used for crystallization. Both the crystallization solvent and the structural restraints imposed by the crystal lattice may have a major effect on the kinetics, on the populations of intermediates, and even on the quantum yield for photoinitiation. It is therefore highly desirable to compare the kinetics in solution using standard buffer; in crystallization buffers; in a polycrystalline slurry of microcrystals; and in single crystals of dimensions and quality suitable for X-ray analysis. Comparison of the first with the second establishes the effect of the altered solvent required for crystal growth and stability; comparison of the second with the third, the effect of the intermolecular lattice forces and of steric hindrance; and comparison of the third with the fourth, crystal size effects. As an early example of this type of study, kinetic studies by flash photolysis of ligand binding to haemoglobin (Parkhurst & Gibson 1967) established the similarity of the reaction in solution and in the crystal and hence the validity of using the crystal structures to interpret the solution data.

It should be emphasized that optical monitoring may not reveal all structural intermediates. While we might expect the rate constants derived from optical monitoring of crystals to appear in the time-dependence of the X-ray intensities also (Moffat 1989), this is not necessarily the case. A particular optical intermediate may involve only a minor electronic rearrangement of a chromophore which is loosely coupled to its protein environment, and thus be undetectable by X-ray techniques; and conversely, there may be protein structural rearrangements which are not directly detectable by optical techniques.

In addition to these off-line studies, it is highly desirable to be able to monitor the optical properties of a particular crystal on-line while it is being used for the X-ray studies. That is, a single crystal microspectrophotometer must be combined with an X-ray camera. A block diagram of such an apparatus which we have constructed is shown in figure 2. Single crystal studies are prone to light scattering and other artefacts, whose effects can be identified and minimized by using a white light source and a multi-wavelength, diode array detector to accumulate a broad-band spectrum. Since a spectrum can be acquired in 0.5 ms, the microspectrophotometer is also suitable for kinetic studies on this timescale.

#### *(d) X-ray monitoring*

An ideal X-ray detector for time-resolved experiments would possess all the desired attributes of a conventional detector and in addition, the ability to acquire, initially process and store X-ray images at all frequencies from DC up to the X-ray pulse frequency. No present, or even contemplated, detector comes close to these requirements. The fundamental problem lies in the data acquisition rate rather than in the data extent (Gruner 1987). For example, an individual storage phosphor image contains 10 Mbytes of information which at 1 MHz corresponds to 10 Tbytes per second.

Since an ideal photon counting detector for time-resolved crystallography is

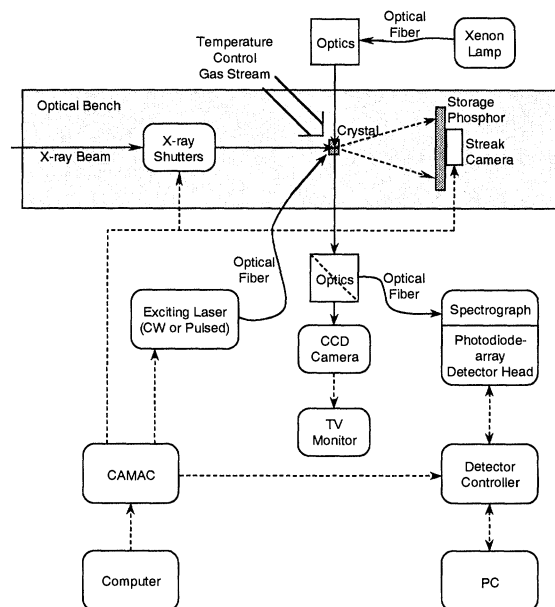


Figure 2. Block diagram of X-ray and optical apparatus for time-resolved crystallography.

lacking, most data have been collected using integrating detectors such as image plates, storage phosphors or even film. The time dimension is introduced either by rapid interchange of cassettes (Amemiya *et al.* 1987) in which each time point is recorded on a separate image, or by moving the cassette in its plane during the exposure so as to lay down a series of time points on a single image (Moffat 1989).

Illumination of a crystal by an intense X-ray beam causes heating and radiation damage due to X-ray absorption, which will be non-uniform if the crystal is strongly absorbing at the wavelengths of interest. The key factor is not the rate of temperature rise, but the extent of temperature rise during the X-ray exposure, its variation with position in the crystal, and its effect on molecular structure and the crystal lattice. Helliwell (1992) calculates the rates of temperature rise for typical monochromatic X-ray beams and shows that the extent of temperature rise is not a serious problem. The extent of temperature rise is, however, much larger for typical polychromatic, Laue beams, and particularly for time-resolved experiments where the total exposure is given by the exposure per time point multiplied by the number of time points. As noted above, if X-ray exposures are shorter than roughly 50 ms, little or no thermal equilibration can occur across the crystal, or between the crystal and its surroundings. Irrespective of the temperature of the crystal or the efficiency of crystal cooling by an external gas stream, heat generated in the interior of the crystal by X-ray absorption cannot be appreciably dissipated by conduction to the surface during the exposure. For example, we have found that a single 100 ms exposure of a PYP crystal using the intense, focused white beam spanning 7–17 keV on bending magnet beam line X26C at the National Synchrotron Light Source (NSLS) produces diffraction maxima with substantially increased apparent mosaicity; but if the same total exposure is delivered in 10 sub-exposures of 10 ms each, separated by 90 ms to allow thermal equilibration, the mosaicity is greatly reduced. We calculate that a single 100 ms exposure heats the front of the crystal by 8.5 °C



and the back by 7.3 °C; this is evidently sufficient to distort this crystal lattice and introduce mosaicity. The process is reversible and cannot therefore be attributed to the chemical radiation damage produced by free radical generation. The diffusion of free radicals is inhibited by freezing, and hence chemical radiation damage can be minimized by working at cryogenic temperatures (Watenpaugh 1991).

(e) *Data analysis*

In an ideal experiment, the reciprocal lattice is perfect and time-invariant; all molecules behave independently of one another and conformers are distributed spatially at random in the crystal; the space-average contents of the unit cell and their continuous molecular transform evolve smoothly with time, and may be represented by a sum of exponentials; the time course of the intensity of each diffraction spot is also represented by a sum of exponentials in which the exponents are identical for all reflections but the amplitudes of each exponential vary from reflection to reflection; and both the time-dependent, space-average structure and its individual, time-independent structural components, each arising from a particular intermediate, may be extracted, by the strategy advocated by Moffat (1989).

How does reality differ? First, in any crystal undergoing a structural reaction in which the molecular conformations are not rigidly correlated, there will be time periods in which the crystal is structurally heterogeneous, and in which the (at least local) direct lattice may differ from the initial state. Thus we have to consider the sampling of an average continuous transform by a disordered reciprocal lattice. If the rate constants governing the conformational changes are suitably dispersed, there may also be time periods in which the molecular conformation and the lattice are spatially uniform; an example of this particularly favourable case is given below for PYP (§3*a*). Secondly, the representation of the time dependence for the molecular transform as a sum of exponentials is not essential; the point is that the populations of the individual conformations must evolve with time in a defined manner. Thirdly, there may be some correlation of conformation (or position) between nearby molecules, as evidenced by the diffuse scattering which certain crystals exhibit even in their static diffraction patterns (Doucet & Benoit 1987; Caspar *et al.* 1988; Caspar & Badger 1991). Fourthly, thermal gradients and other conformational gradients will occur unless precautions are taken to minimize them, and will result in spatial gradients in the continuous molecular transform and in the reciprocal lattice which may resemble apparent mosaicity. Further, the gradients may be time-dependent and hence confused with the desired target, the time-dependent continuous molecular transform.

These problems are just beginning to be tackled. Our understanding of static and dynamic disorder in protein crystals, whatever its source, is limited. However, it is worth pointing out that extensive, substitutional disorder analogous to that in a time-resolved experiment is always present in any partly occupied, multiple site, heavy atom derivative, yet does not preclude the use of this derivative in phasing.

### 3. Results

(a) *Photoactive yellow protein*

Almost all time-resolved crystallographic studies to date have concentrated on slow reactions, where intermediate formation and breakdown is measured in minutes or longer (Hajdu *et al.* 1987; Schlichting *et al.* 1990; Singer *et al.* 1992). Slower

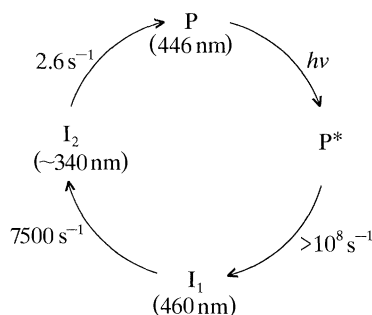


Figure 3. The photocycle of PYP, based on data in Meyer *et al.* (1989).

reactions allow longer exposure times and lower incident X-ray intensities, which minimize thermal artifacts induced by X-ray absorption gradients. Reaction initiation can proceed via diffusion or slow, repeated flash lamp photoinitiation, which minimizes spatial and light-induced thermal gradients. We have instead concentrated on faster reactions with short-lived intermediate states lasting for seconds or much less, and have encountered a series of unexpected difficulties.

One such system is photoactive yellow protein, PYP, a small soluble, 14 KDa photoreceptor protein with a fully reversible photocycle resembling that of sensory rhodopsin. The crystal structure of PYP isolated from the halophilic bacterium *Ectothiorhodospira halophila* (Meyer 1985) has been determined at 2.4 Å† resolution (McRee *et al.* 1989) and refinement to a resolution of less than 2 Å is under way. The chromophore is believed to be retinal-like, but its identity has not been established. Immediate bleaching of its yellow colour by a laser pulse is followed by further bleaching on a much slower timescale, and finally by recovery of the initial spectrum over several seconds.

The PYP system is nearly ideal for rapid time-resolved studies. The crystals are of known structure, of low mosaic spread, scatter X-rays strongly to around 1.4 Å resolution, and are relatively resistant to radiation damage, both from synchrotron X-rays and from pulsed and CW lasers. PYP crystallizes in a high symmetry, hexagonal space group of moderate cell dimensions (McRee *et al.* 1986) that allows the unique data to be collected on only a small number of Laue images, and avoids Laue spot overlap problems (Cruickshank *et al.* 1991). The kinetics of the photocycle (Meyer *et al.* 1987, 1989) reveal a series of spectrally distinct intermediates which decay via first order reactions (figure 3) and whose lifetimes are quite different, so that there are time periods when the crystal is essentially homogeneous (figure 4). Since all reactions are unimolecular, the high protein concentration in the lattice, 63 mM, is of no (kinetic) consequence and diffusion problems are absent. However, the closely-packed lattice may restrict the conformational changes which indirect evidence suggests (Meyer *et al.* 1989) accompanying photocycling. The quantum yield for photoinitiation in solution is high, 0.64 (Meyer *et al.* 1989), although polycrystalline slurries of microcrystals and single crystals of X-ray dimensions appear somewhat harder to bleach. The photocycle appears to be fully reversible, which may permit X-ray data to be accumulated over many cycles if necessary. Finally, PYP appears to be a particularly simple photoreceptor and as such, is of considerable biophysical interest.

$$\dagger 1 \text{ \AA} = 10^{-10} \text{ m} = 10^{-1} \text{ nm.}$$

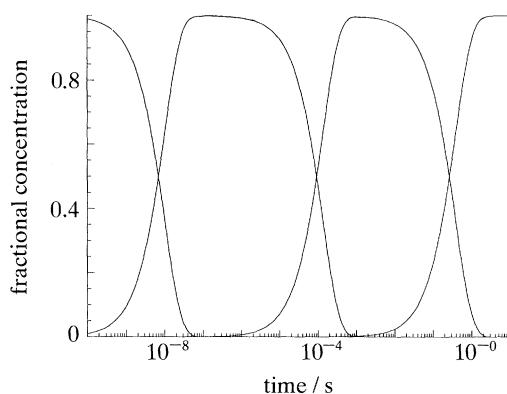


Figure 4. Fractional occupancy versus time for intermediates in the photocycle of PYP. Rate constants used are  $10^8 \text{ s}^{-1}$ ,  $7500 \text{ s}^{-1}$  and  $2.6 \text{ s}^{-1}$  as in figure 3.

We have studied the optical properties of PYP crystals using a single crystal microspectrophotometer in order to design time-resolved crystallographic experiments. Since the protein concentration in the crystals is high and the extinction coefficient in solution at the absorption maximum of 445 nm is also high,  $48 \text{ mM}^{-1} \text{ cm}^{-1}$ , crystals have a very high optical density at 445 nm. To allow 87% or more of the light to be transmitted through a crystal of  $50 \mu\text{m}$  thickness (thus minimizing absorption and thermal gradients), the extinction coefficient at the initiating wavelength must be less than  $0.2 \text{ mM}^{-1} \text{ cm}^{-1}$ . We find that the crystals have an absorption maximum at 450 nm, slightly red-shifted from solution, and exhibit pronounced linear dichroism. The absorption of the crystals can be greatly reduced by working on the long wavelength end of the 450 nm band, using for example Ar ion laser lines at 488 or 496.5 nm, and by using plane-polarized radiation where the orientation of the plane of polarization with respect to the crystal axes is controlled.

Since PYP has a long-lived intermediate (figure 3), a bleached photostationary state can be readily established via continuous illumination with a relatively low power CW laser. In such experiments, clear optical evidence for bleaching of small single crystals was obtained by illumination with a CW Ar laser at 488 and 496.5 nm, but not at 514 nm where the crystals are completely transparent. The spectral changes saturated as the laser power was increased, and were reversible (data not shown). When these experiments were repeated using slightly larger crystals illuminated by the CHESS X-ray beam or the NSLS X26C beam described earlier, an increase in mosaic spread was seen whenever the laser fell on the crystals (figure 5). The increase rapidly and completely disappeared when the laser was shut off. The mosaicity was not uniformly evident in reciprocal space; and qualitatively, most reflections were of lower peak intensity when the laser was on. If a true photostationary state were established in which almost all molecules were in the long-lived intermediate conformation, then some reflections would be expected to increase in integrated intensity, some to remain unchanged, and some to decrease, relative to the initial, ground state. Quantitative analysis showed this to be the case. A similar, transient increase in mosaicity had been seen earlier when crystals of PYP were stimulated by a pulsed laser (data not shown).

An understanding of these effects must be based on the photochemistry in the

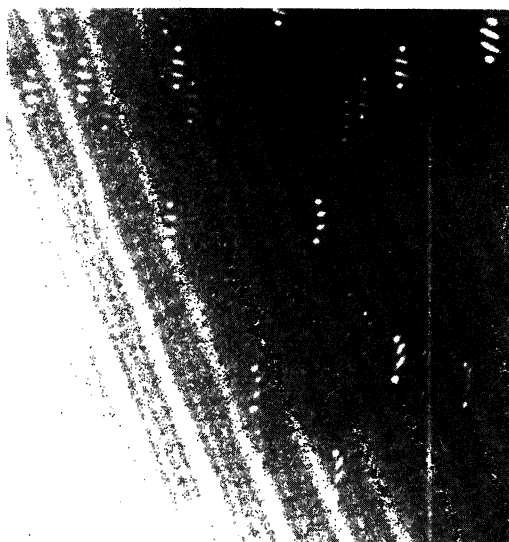


Figure 5. A portion of the Laue pattern of a PYP crystal, obtained with the streak camera. Top spots, laser off; second spot, 10 mW CW Ar ion laser on for 5 s; third spot, laser on for a further 10 s; bottom spot, laser off for 30 s.

crystal. We have developed a model which describes the laser intensity and degree of photobleaching as a function of time and of position in the crystal. Representative calculations based on this model are shown in figure 6. If a laser wavelength is chosen where the extinction coefficient is low (figure 6 *a-f*), then gradients of bleaching and temperature are minimized; but if in addition the laser power is too low to achieve complete bleaching, then the overall temperature rise is large (compare figure 6*d* with figure 6*b*). If an inappropriate laser wavelength is chosen where the extinction coefficient is high, then very large gradients of bleaching and temperature are produced (figure 6*g,h*). The model suggests that the appropriate conditions for CW laser illumination are those shown in figure 6*c,d*, and for pulsed laser illumination, those in figure 6*e, f*. Experiments to evaluate this model are in progress.

#### (b) 120 ps X-ray exposures

Can X-ray diffraction patterns be obtained from single crystals using the 120  $\mu\text{s}$  pulse of X-rays emitted by a single bunch of electrons or positrons as they traverse a hard X-ray undulator? If so, can structure amplitudes sufficiently precise and numerous for crystallographic structure determination be obtained? In June 1988, the CHESS/Argonne undulator, a prototype for the APS undulator A (Bilderback *et al.* 1989; Shenoy *et al.* 1988) was inserted in the Cornell Electron-Positron Storage Ring CESR. Using it, we demonstrated (Szebenyi *et al.* 1988, 1992) that such patterns can indeed be obtained and quantitated, for large crystals of the scattering power of an indole alkaloid and lysozyme. However, only a small fraction of the predicted spots were in fact observed (29–42% for the alkaloid and 2–7% for lysozyme) due to insufficient spectral intensity and the exceedingly brief exposure. The maximum value of the spectral intensity at the peak of the third undulator harmonic at 0.97  $\text{\AA}$  was calculated for a 300  $\mu\text{m}$  collimator to be  $9 \times 10^9$  photons  $(\text{s mA } 0.1\% \text{ bandpass})^{-1}$ , or  $7.5 \times 10^5$  photons  $(0.1\% \text{ bandpass})^{-1}$  per bunch at a CESR single bunch current of 32.5 mA (Szebenyi *et al.* 1992). From these results we

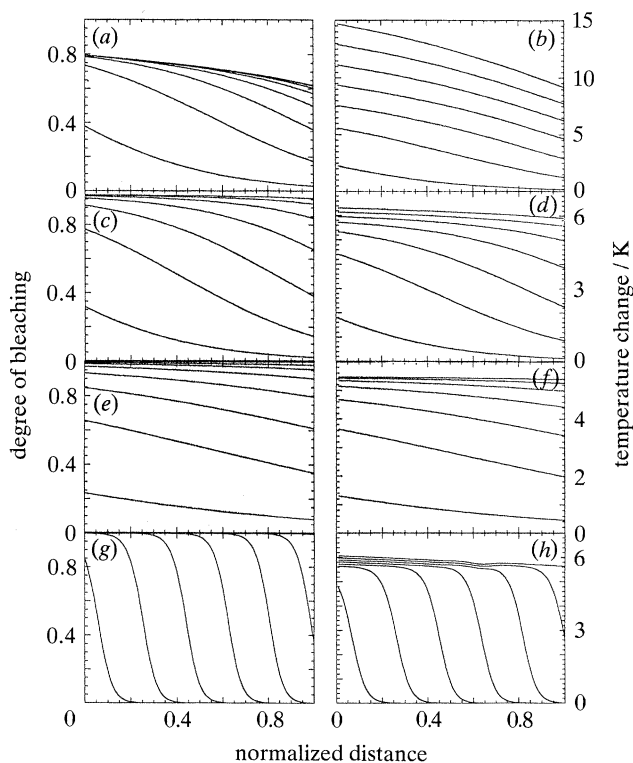


Figure 6. The effects of laser power density ( $P$ ) and extinction coefficient ( $\epsilon$ ) on crystal bleaching and the associated rise in temperature, as a function of position in the crystal. The degree of bleaching (left column) and the temperature change (right column) are shown for four cases. Each panel shows a time sequence of the approach to the photostationary state. The crystal thickness (0.1 mm), quantum yield (0.64), and rate constant ( $3.3 \text{ s}^{-1}$ ) are the same for all four cases. Case 1 (a) and (b): CW laser,  $P = 10 \text{ mW mm}^{-2}$ ,  $\epsilon = 4.8 \text{ mm}^{-1} \text{ cm}^{-1}$ , time interval between curves is 40 ms; case 2 (c) and (d): CW laser,  $P = 100 \text{ mW mm}^{-2}$ ,  $\epsilon = 4.8 \text{ mm}^{-1} \text{ cm}^{-1}$ , time interval between curves is 3 ms; case 3 (e) and (f): pulsed laser,  $P = 10 \text{ mJ } \mu\text{s}^{-1} \text{ mm}^{-2}$ ,  $\epsilon = 4.8 \text{ mm}^{-1} \text{ cm}^{-1}$ , time interval between curves is 0.05  $\mu\text{s}$ ; case 4 (g) and (h): CW laser,  $P = 100 \text{ mW mm}^{-2}$ ,  $\epsilon = 48 \text{ mm}^{-1} \text{ cm}^{-1}$ , time interval between curves is 1.5 ms.

estimate that a two to three orders of magnitude greater spectral intensity will be necessary to record most of the predicted spots for a crystal of the scattering power of lysozyme in 120 ps. That is, from  $10^8$ – $10^9$  photons  $(0.1\% \text{ bandpass})^{-1}$  per bunch is required, for a 300  $\mu\text{m}$  collimator. Is this attainable? The calculated value of the spectral intensity at 20 keV for a focused wiggler beam at the ESRF, delivered through a smaller  $200 \times 200 \mu\text{m}$  aperture, is  $1.8 \times 10^7$  photons  $(0.1\% \text{ bandpass})^{-1}$  per bunch at a single bunch current of 7.5 mA (Wulff 1991): tantalizingly close to that required. A value of  $10^8$  photons  $(0.1\% \text{ bandpass})^{-1}$  may indeed be attainable with this beamline, and with its counterpart at the APS.

In July 1991, the CHESS/Argonne undulator was inserted for the second time into CESR. We wanted to solve an unknown structure using 120 ps data, and thus to demonstrate that crystallography is feasible on this timescale. To that end, in collaboration with M. Szebenyi, J. R. Steiner and J. Clardy (Cornell University, U.S.A.), we collected 120 ps Laue data on crystals of a complex natural product denoted briarane B, a diterpenoid. 18 images were obtained at  $10^\circ$  rotation intervals

using the Kodak storage phosphor detector, the ultrafast shutter (LeGrand *et al.* 1989), and CESR single bunch currents up to 49 mA. The crystals are in space group  $P2_1$ ,  $a = 11.086$ ,  $b = 8.242$ ,  $c = 15.864$  Å,  $\beta = 91.68^\circ$ , as determined from a conventional diffractometer data-set obtained later with  $\text{CuK}\alpha$  radiation. Processing of the Laue images using the generalized scale factor approach to wavelength normalization (Smith Temple 1989; Szebenyi *et al.* 1992) led to a Laue data-set of 704 unique reflections to 1.1 Å resolution which is 52.4% complete overall. However, it is 0% complete at resolutions lower than 5.5 Å due to the non-uniform sampling of reciprocal space in the Laue technique.

Three data-sets were compared: the complete  $\text{CuK}\alpha$  data-set; a selected  $\text{CuK}\alpha$  data-set containing only the 704 unique reflections present in the Laue set; and the 120 ps Laue set. The structure of briarane B could be solved by direct methods using the SHELXS program from the first data-set, but not from the second or third. However, the structure could readily be refined against the second or third data-sets. We tentatively conclude that the failure to solve the structure using the 120 ps Laue set results from the systematic incompleteness of the data rather than its poor quality. Although we did not succeed in our original aim, the prospects for crystallography on the 100 ps timescale look bright.

#### 4. Conclusions

Time-resolved crystallography continues to face experimental challenges, not least of which is the identification of crystal systems in which biological activity and the associated structural changes are permitted, while crystal quality sufficient for application of the Laue technique is maintained. There almost certainly are systems for which these requirements cannot simultaneously be met. A second major challenge, particularly when rapid reactions are to be studied, comes in devising and applying suitable reaction initiation techniques, in a manner that avoids unnecessary gradients of concentration, temperature and cell dimensions. Careful attention to the optical properties of the crystals and to the photochemistry of the initiation reaction will meet this challenge, for most systems. Time-resolved crystallography is unlikely ever to be straightforward; but the rewards from successful experiments, in terms of a solid understanding of mechanism, are likely to warrant the effort.

We thank Jon Clardy for crystals of briarane B; Marian Szebenyi and Jorge L. Rios Steiner for data analysis on briarane B; Wilfried Schildkamp, Alan LeGrand, Tsu-Yi Teng, Zhong Ren, Claude Pradervand, Mark Rivers, Keith Jones, Grace Shea McCarthy, Hans Parge and Cindy Sodini for technical assistance in connection with synchrotron experiments; and Patrick Burke and Che-fu Kuo for help with crystal preparation of PYP. Supported by NIH grant GM 36452 to K.M., GM 37684 to E.D.G., and a grant from the Keck Foundation.

#### References

- Amemiya, Y., Wakabayashi, K., Tanaka, H., Ueno, Y. & Miyahara, J. 1987 Laser-stimulated luminescence used to measure X-ray diffraction of a contracting striated muscle. *Science, Wash.* **237**, 164–168.
- Amorós, J. L., Buerger, M. J. & Amorós, M. C. 1975 *The Laue method*. New York: Academic Press.
- Bilderback, D. H., Batterman, B. W., Bedzyk, M. J., Finkelstein, K., Henderson, C., Merlini, A., Schildkamp, W., Shen, Q., White, J., Blum, E. B., Viccaro, P. J., Mills, D. M., Shenoy, G. K., Robison, K. E., James, F. E. & Slater, J. M. 1989 Performance of a hard X-ray undulator at CHESS. *Rev. scient. Instrum.* **60**, 1419–1425.

*Phil. Trans. R. Soc. Lond. A* (1992)

- Caspar, D. L. D. & Badger, J. 1991 Plasticity of crystalline proteins. *Curr. Opin. struct. Biol.* **1**, 877–882.
- Caspar, D. L. D., Clarage, J., Salunke, D. M. & Clarage, M. 1988 Liquid-like movements in crystalline insulin. *Nature, Lond.* **332**, 659–662.
- Cruikshank, D. W. J., Helliwell, J. R. & Moffat, K. 1991 Angular distribution of reflections in Laue diffraction. *Acta crystallogr.* **A47**, 352–373.
- Doucet, J. & Benoit, J. P. 1987 Molecular dynamics studied by analysis of the X-ray diffuse scattering from lysozyme crystals. *Nature, Lond.* **325**, 643–646.
- Gruner, S. 1987 Time-resolved X-ray diffraction of biological materials. *Science, Wash.* **238**, 305–312.
- Gutfreund, H. & Knowles, J. R. 1967 The foundations of enzyme action. *Essays Biochem.* **3**, 25–72.
- Hajdu, J. & Johnson, L. N. 1990 Progress with Laue diffraction on protein and virus crystals. *Biochem.* **29**, 1669–1678.
- Hajdu, J., Machin, P. A., Campbell, J. W., Greenhough, T. J., Clifton, I. J., Zurek, S., Gover, S., Johnson, L. N. & Elder, M. 1987 Millisecond X-ray diffraction: first electron density map from Laue photographs of a protein crystal. *Nature, Lond.* **329**, 178–181.
- Helliwell, J. R. 1985 Protein crystallography with synchrotron radiation. *J. molec. Struct.* **130**, 63–91.
- Helliwell, J. R. 1992 *Macromolecular crystallography and synchrotron radiation*. Cambridge University Press.
- Kaplan, J. H., Forbush, B. & Hoffman, J. F. 1978 Rapid photolytic release of adenosine 5'-triphosphate from a protected analogue: utilization by the Na<sup>+</sup>: K<sup>+</sup> pump of human red blood cell ghosts. *Biochem.* **17**, 1929–1935.
- LeGrand, A. D., Schildkamp, W. & Blank, B. 1989 An ultrafast mechanical shutter for X-rays. *Nucl. Instrum. Meth.* **A275**, 442–446.
- Makinen, M. W. & Fink, A. L. 1977 Reactivity and cryoenzymology of enzymes in the crystalline state. *A. Rev. Biophys. Bioengng* **6**, 301–343.
- Margaritondo, G. 1988 *Introduction to synchrotron radiation*. New York and Oxford: Oxford University Press.
- McCray, J. A. & Trentham, D. R. 1989 Properties and uses of photoreactive caged compounds. *A. Rev. Biophys. biophys. Chem.* **18**, 239–270.
- McRee, D. E., Tainer, J. A., Meyer, T. E., Van Beeumen, J., Cusanovich, M. A. & Getzoff, E. D. 1989 Crystallographic structure of a photoreceptor protein at 2.4 Å resolution. *Proc. natn. Acad. Sci. U.S.A.* **86**, 6533–6537.
- McRee, D. E., Meyer, T. E., Cusanovich, M. A., Parge, H. E. & Getzoff, E. D. 1986 Crystallographic characterization of a photoactive yellow protein with photochemistry similar to sensory rhodopsin. *J. biol. Chem.* **261**, 13850–13851.
- Meyer, T. E. 1985 Isolation and characterization of soluble cytochromes, ferredoxins and other chromophoric proteins from the halophilic phototrophic bacterium, *Ectothiorhodospira halophila*. *Biochim. biophys. Acta* **806**, 175–183.
- Meyer, T. E., Yakali, E., Cusanovich, M. A. & Tollin, G. 1987 Properties of a water-soluble yellow protein isolated from a halophilic phototrophic bacterium that has photochemical activity analogous to sensory rhodopsin. *Biochem.* **26**, 418–423.
- Meyer, T. E., Tollin, G., Hazzard, J. H. & Cusanovich, M. A. 1989 Photoactive yellow protein from the purple phototrophic bacterium, *Ectothiorhodospira halophila*. *Biophys. J.* **56**, 559–564.
- Moffat, K., Szebenyi, D. & Bilderback, D. 1984 X-ray Laue diffraction from protein crystals. *Science, Wash.* **223**, 1423–1425.
- Moffat, K. 1989 Time-resolved macromolecular crystallography. *A. Rev. Biophys. biophys. Chem.* **18**, 309–332.
- Moffat, K., Bilderback, D., Schildkamp, W., Szebenyi, D. & Teng, T.-Y. 1989 Laue photography from protein crystals. In *Synchrotron radiation in structural biology* (ed. R. M. Sweet & A. D. Woodhead), pp. 325–330. New York: Plenum Press.
- Parkhurst, L. J. & Gibson, Q. H. 1967 The reaction of carbon monoxide with horse hemoglobin in solution, in erythrocytes and in crystals. *J. biol. Chem.* **242**, 5762–5770.

- Schlichting, I., Almo, S. C., Rapp, G., Wilson, K., Petratos, K., Lentfer, A., Wittinghofer, A., Kabsch, W., Pai, E. E., Petsko, G. A. & Goody, R. S. 1990 Time-resolved X-ray crystallographic study of the conformational change in Ha-Ras p21 protein on GTP hydrolysis. *Nature, Lond.* **345**, 309–315.
- Schulz, G. E. 1991 Domain motions in proteins. *Curr. Opin. struct. Biol.* **1**, 883–888.
- Shenoy, G. K., Viccaro, P. J. & Mills, D. M. 1988 *Characteristics of the 7 GeV Advanced Photon Source, a guide for users*. Argonne National Laboratory Publication ANL-88-9, Argonne, Illinois.
- Smith Temple, B. 1989 Extraction of structure factor amplitudes from Laue X-ray diffraction images. Ph.D. thesis, Cornell University, Ithaca, New York, U.S.A.
- Smither, R. K. & Freund, A. K. 1990 *Workshop on High Heat Load X-Ray Optics*. Argonne Publication ANL/APS/KM-6, Argonne National Laboratory.
- Szebenyi, D. M. E., Bilderback, D., LeGrand, A., Moffat, K., Schildkamp, W. & Teng, T.-Y. 1988 120 picosecond Laue diffraction using an undulator X-ray source. *Trans. Am. crystallogr. Assoc.* **24**, 167–172.
- Szebenyi, D. M. E., Bilderback, D. H., LeGrand, A., Moffat, K., Schildkamp, W., Smith Temple, B. & Teng, T.-Y. 1992 Quantitative analysis of Laue diffraction patterns recorded with a 120 picosecond exposure from an X-ray undulator. *J. appl. Crystallogr.* **25**, 414–423.
- Watenpaugh, K. D. 1991 Macromolecular crystallography at cryogenic temperatures. *Curr. Opin. struct. Biol.* **1**, 1012–1015.
- Wood, I. G., Thompson, P. & Matthewman, J. C. 1983 A crystal structure refinement from Laue photographs taken with synchrotron radiation. *Acta crystallogr B* **39**, 543–547.
- Wulff, M. 1991 The Laue beamline. *ESRF Newslett.* **10**, 7–9.
- Wyckoff, H. W., Doscher, M., Tsernoglou, D., Inagami, T., Johnson, L. N., Hardman, K. D., Allewell, N. M., Kelly, D. M. & Richards, F. M. 1967 Design of a diffractometer and flow cell system for X-ray analysis of crystalline proteins with application to the crystal chemistry of ribonuclease S. *J. molec. Biol.* **27**, 563–578.

### Discussion

M. ROSSMANN (*Purdue University, Indiana, U.S.A.*). Would you comment on the use of monochromatic versus polychromatic radiation for time-resolved studies?

KEITH MOFFAT. There certainly are circumstances where monochromatic data collection is preferable to Laue: crystals of high radiation sensitivity, of high symmetry such that a small number of oscillation photographs yield a chemically interpretable difference Fourier, or undergoing a slow reaction with intermediate lifetimes of several minutes. However, the Laue technique is more appropriate for study of faster reactions with intermediate lifetimes well under one second. The optimum bandpass for time-resolved data collection will depend on the crystal. For some such as rhino virus, it may be  $10^{-3}$  Å (monochromatic); for others, it may be 0.3 Å (narrow bandpass Laue); and for yet others such as PYP, it may be 1.5 Å (wide bandpass Laue).

J. HAJDU (*Oxford University, U.K.*). (i) Did you obtain any structural information from the Laue photographs of the yellow protein? How complete is the data-set? (ii) Why do you use multiple exposures on the same imaging plate? This is detrimental to data as background is additive on the picture.

K. MOFFAT. (i) No. Our strategy at this time is to identify the sources of the spot streakiness and to minimize (or eliminate) them, before collection of complete data-sets. (ii) The background is indeed increased by a factor equal to the number of exposures. However, the structural information lies in the small intensity differences



between time points. Their accurate measurement is affected by random errors (for example, those that arise from enhanced background) and by systematic errors (for example, those that arise from scaling together separate images, one from each time point). Multiple exposures on the same imaging plate depend on the trade-off between these sources of error, and on other factors such as the extent of spot overlap, the minimum interval between time points, and so forth.

G. A. PETSKO (*Brandeis University, Massachusetts, U.S.A.*). In your small molecule study, did you try any computational tricks to compensate for the systematically missing data? We found that this same problem prevented us from solving heavy atom difference Patterson maps in protein Laue studies, but that it could be overcome – to some extent – by, for example, subtracting the point spread function Patterson.

K. MOFFAT. This is a good idea; we've not tried it yet.

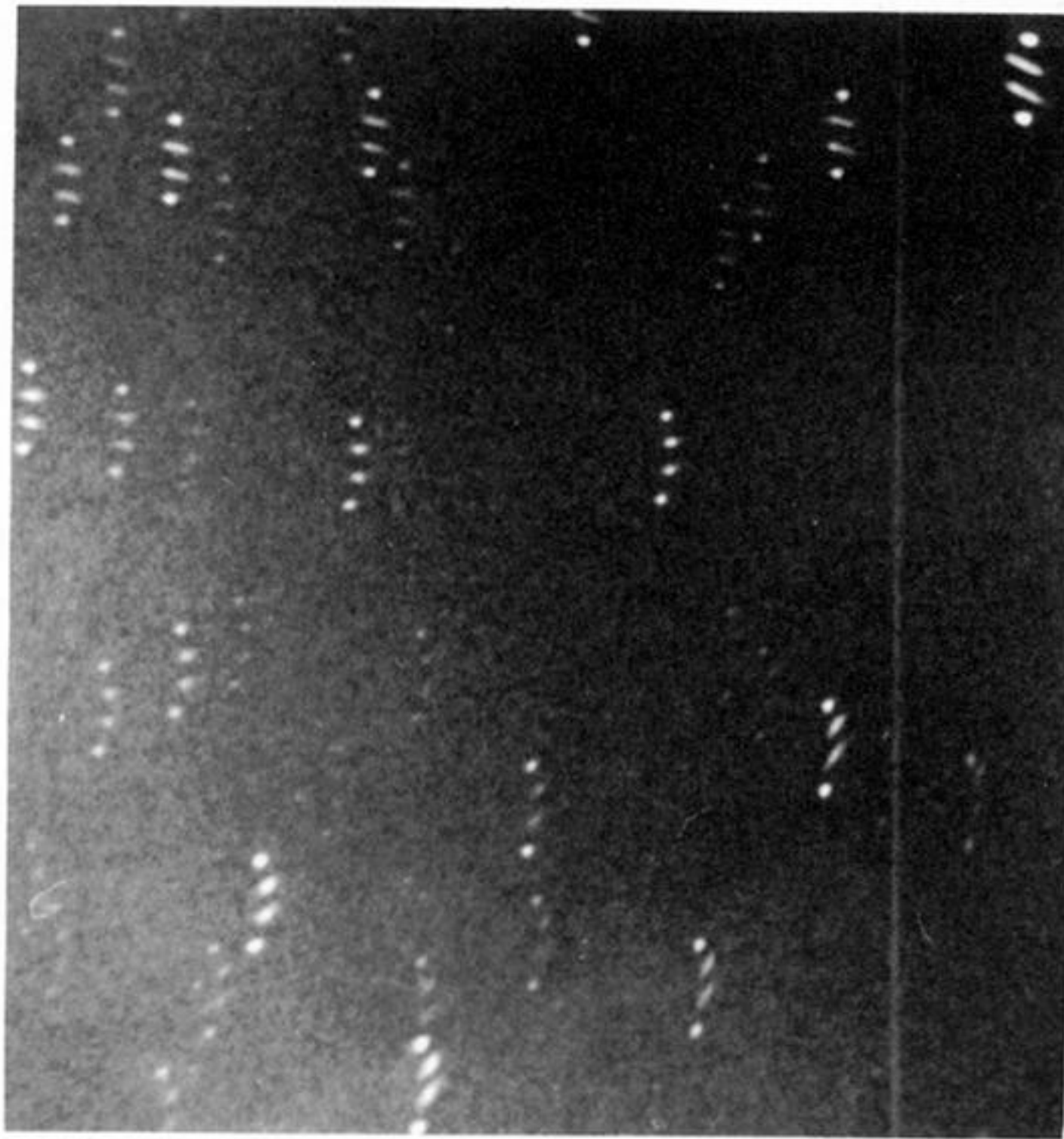


Figure 5. A portion of the Laue pattern of a PYP crystal, obtained with the streak camera. Top spots, laser off; second spot, 10 mW CW Ar ion laser on for 5 s; third spot, laser on for a further 10 s; bottom spot, laser off for 30 s.